

Mineralogy of the Light-Toned Outcrop Rock at Meridiani Planum as seen by Mini-TES. T. D. Glotch¹, J. L. Bandfield², P. R. Christensen², W. M. Calvin³, S. M. McLennan⁴, B. C. Clark⁵, and the Athena Science Team
¹California Institute of Technology, tglotch@gps.caltech.edu, ²Arizona State University, ³University of Nevada Reno, ⁴SUNY Stonybrook, ⁵Lockheed Martin Space Systems

Introduction: The Opportunity rover landed in Eagle Crater in Meridiani Planum on January 24, 2004. Among the first images acquired included a light-toned rock that was the first outcrop observed from the surface of Mars. As seen in Pancam and Microscopic Imager images [1,2], the outcrop rock is layered, and portions exhibit fine-scale morphology similar to terrestrial ripple marks [3]. The outcrop rock is also the source of the nearly ubiquitous hematite-rich spherules, which can be seen eroding out of the outcrop [2,4]. Initial in-situ analyses of the rock by the Alpha Particle X-ray Spectrometer (APXS) showed high levels of sulfur correlated with magnesium, suggesting the presence of magnesium sulfates [5]. This result was confirmed by the Miniature Thermal Emission Spectrometer (Mini-TES), which has also seen evidence for calcium sulfates [6]. Additionally, measurements by the Mössbauer spectrometer have indicated that the outcrop is composed of ~10% jarosite, a ferric iron sulfate [7]. In this work, we expand on the initial Mini-TES analyses of the light-toned outcrop rock [6,8], using the results of the APXS and Mössbauer instruments to constrain mineral deconvolution models. We also examine Mini-TES spectra of fines derived from the outcrop rock by application of the Rock Abrasion Tool (RAT) [9,10] and compare these spectra to that of the globally homogenous fines (GHF).

Methods: [8] used factor analysis and target transformation techniques to determine the independently varying components in the scene viewed by Mini-TES at Meridiani Planum. Seven spectral shapes were derived including hematite, surface dust, basaltic sand, outcrop rock, two atmospheric shapes, and blackbody. A spectral library consisting of silicate, sulfate, and oxide endmembers was used to deconvolve the outcrop spectral shape. The deconvolution model was constrained by the results of previous analyses of APXS [5,11,12] and Mössbauer [7] data as well as Mini-TES observations of outcrop-derived fines. Specifically, three constraints were placed on the deconvolution model: (1) the natrojarosite endmember was forced to be ~10% of the total rock, based on estimates from the Mössbauer and APXS instruments [5,7,11], (2) the spectral contrast of Mg- and Ca-bearing sulfates were adjusted to take into account the Mg/Ca ratio available for placement in sulfates [11,12], (3) carbonates are not included in the library based on Mini-TES observations of outcrop-derived

fines. When these constraints are not imposed, natrojarosite, Mg- and Ca-bearing sulfates are all still used in the model.

In addition to deconvolution of the outcrop rock spectral shape, we examined long-dwell Mini-TES stares of the Guadalupe and McKittrick outcrop targets in Eagle crater after application of the RAT. The resulting observations were dominated by outcrop-derived fines with average particle sizes comparable to the GHF [10]. The spectra of the outcrop derived fines are compared to the globally homogenous dust spectrum derived from Mini-TES data by [8].

Results and Discussion:

The most noticeable difference between the GHF and the outcrop fines spectra (Figure 1) occurs in the region $>1250\text{ cm}^{-1}$. The GHF spectrum has an overall increased emissivity compared to the outcrop fines between ~ 1300 and 1600 cm^{-1} , with local emissivity minima at 1400 and 1600 cm^{-1} . This structure has been attributed to the presence of carbonates at the 2-5% level [13]. An alternative view is that this structure is indicative of the presence of hydrous iron sulfates [14]. Regardless of the nature of the absorbing material in the GHF, detailed laboratory work [13] has shown that the presence of 2-5 wt.% carbonate minerals in a plagioclase dust matrix can cause the structure at $>1250\text{ cm}^{-1}$ seen in the GHF. Thus, the lack of this structure in the outcrop-derived fines is indicative that carbonate concentration in the outcrops is significantly less than 2-5 wt.%, and probably zero.

The results of the deconvolution of the target transformation-derived outcrop rock spectral shape are shown in Figure 2 and Table 1. Results from the deconvolution indicate that the outcrop rock is composed primarily of sulfates and amorphous silica/glass/smectite. Amorphous silica and glass are modeled at 25% abundance. In addition, a smectite phyllosilicate (nontronite) is modeled at 10%. Additional components of plagioclase feldspar (15%), hematite (5%), and quartz (5%) are also modeled, although the hematite and quartz abundances are below the Mini-TES detection limit and are not reliable. The Mg-bearing sulfate used in the deconvolution is kieserite ($\text{MgSO}_4 \cdot \text{H}_2\text{O}$), which is modeled at an abundance of 20%. The Ca-bearing sulfate is anhydrite (CaSO_4), which is modeled at 10% abundance, although preliminary tests with a separate simultaneous solution least squares deconvolution model indicates that the Ca-bearing sulfate composition may be composed of both anhydrite and bassanite ($\text{CaSO}_4 \cdot \frac{1}{2}\text{H}_2\text{O}$).

The model fit shown in Figure 2 is relatively good, but can be improved. Additional work must be done to identify phases that can improve the fit at long wavelengths as well as the shoulders of the major absorption feature centered at $\sim 1200\text{ cm}^{-1}$. Relatively few sulfates have been included in the endmember library used in this study due to the lack of availability of suitable spectra, and the inclusion of additional probable sulfate phases may improve the fit

An additional result worthy of future investigation is the inclusion of both amorphous silica/glass and phyllosilicates, specifically nontronite, in the modeled mineralogy of the outcrop rock. Due to the short-ordered nature of amorphous silica, glass, and phyllosilicate crystal structures, these minerals/mineraloids have grossly similar spectra [15,16]. In the deconvolution of the outcrop spectral shape, if either amorphous silica/glass or the nontronite spectra are removed from the endmember library, then the model fit tends to worsen. Recent work [17] has shown that glasses and phyllosilicates are statistically separable in linear deconvolution models. This result strengthens the case that both amorphous silica/glass and smectites may be present in the outcrop rock at Meridiani Planum. Nontronite, an Fe-bearing mineral, is not directly detected by the Mössbauer spectrometer, but [7] report that an unidentified phase referred to as Fe3D3 may be consistent with phyllosilicates.

The correlation of Na and K with Al in APXS measurements of the outcrop rock have led [12] to suggest that unweathered feldspars might be present in the outcrops. This is corroborated by the Mini-TES analysis which shows the presence of 15% plagioclase feldspar. In addition to feldspar, Fe-rich pyroxene has been tentatively detected by the Mössbauer spectrometer. This detection is considered tentative, and could be assigned to a ferrous sulfate [7]. Analysis of the Mini-TES data (Table 2) indicates that no pyroxene is present in the outcrop rock, lending further indirect evidence that the Mössbauer spectrometer may have detected ferrous sulfate rather than pyroxene.

References:

[1]Bell et al. (2004) *Science*, 306, 1703-1708.
 [2]Herkenhoff et al. (2004) *Science*, 306, 1727-1729.
 [3]Grotzinger et al. (2005) *EPSL*, 240, 11-72.
 [4]Soderblom et al. (2004) *Science*, 306, 1723-1726.
 [5]Rieder et al. (2004) *Science*, 306, 1746-1749.
 [6]Christensen et al. (2004) *Science*, 306, 1733-1739.
 [7]Klingelhöfer et al. (2004) *Science*, 306, 1740-1745.
 [8]Glotch et al. (2005) *LPS XXXVI* abstract 2174;
 [9]Gorevan et al. (2003) *JGR*, 108(E12). [10]Bartlett et al. (2005) *LPS XXXVI*, abstract 2292. [11]McLennan et al. (2005) *EPSL*, 240 95-121. [12]Clark et al. (2005) *EPSL*, 240, 73-94. [13]Bandfield et al. (2003) *Science*,

301, 1084-1087. [14]Lane et al. (2004) *GRL*, 31, L19702. [15]Wyatt and McSween (2002) *Nature*, 417, 263-266. [16]Kraft et al. (2003), *GRL*, 30(24), 2288. [17]Koeppen and Hamilton (2005), *JGR*, 110, E08006.

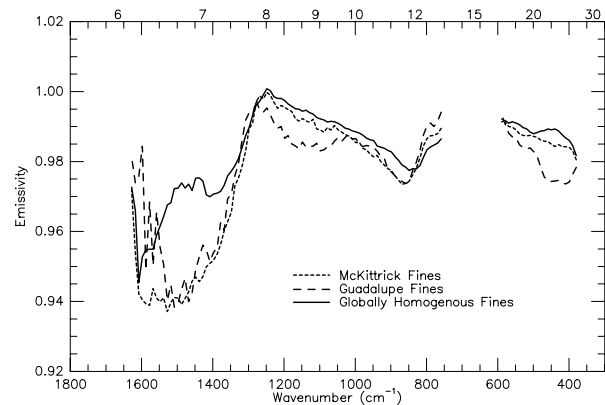


Figure 1. Mini-TES spectra of outcrop-derived fines and the globally homogenous fines. The difference in structure at $>1250\text{ cm}^{-1}$ indicates that the outcrop rock is carbonate-free.

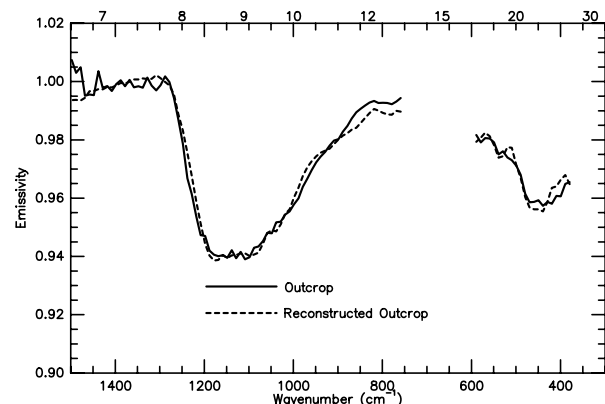


Figure 2. Target transformation-derived outcrop-rock spectral shape and corresponding model fit. Spectral emissivity RMS is 0.307%.

Mineral	Endmem-ber	Base Model
Silica/Glass		25%
Nontronite		10%
Jarosite		10%
Mg-Sulfate		20%
Ca-Sulfate		10%
Plagioclase		15%
Fe-Oxides		5%
Quartz		5%
RMS (%)		0.307

Table 1. Modeled mineralogy of outcrop rock spectral shape.